Research Article

Ebaa Abdulsattar Jaber, Alireza Ataei*, and Ali Tavakoli

Signature verification by geometry and image processing

https://doi.org/10.1515/nleng-2024-0056
received April 26, 2024; accepted November 1, 2024

Abstract: In this article, we present an algorithm to determine the authenticity of a signature with high probability. This study addresses the increasing need for robust and accurate methods of verifying offline signatures, which are crucial in various legal and financial contexts. By combining geometric properties of curves and advanced image processing techniques, our approach effectively distinguishes between genuine and forged signatures. The core of our method utilizes multiple knot B-splines in approximation theory, mean curvature analysis, and curve fitting, providing a comprehensive framework for signature verification. Our findings demonstrate a significant improvement in accuracy over existing methods, as validated by several empirical examples. This research not only contributes to the field of signature verification but also opens avenues for future studies to enhance and adapt our algorithm for broader applications in security and authentication systems.

Keywords: image processing, b-spline, curvature, isogeometry analysis

MSC 2020: 68U10, 65D05, 65G50

1 Introduction

Signature verification is a crucial task in the fields of pattern recognition and security, especially in legal, financial, and administrative contexts where the authenticity of signatures plays a pivotal role. The problem of verifying a signature can be approached in two distinct ways: offline and online verification. Online systems rely on dynamic data such as the pressure, speed, and timing of the signature during its creation, while offline systems work with static images of signatures, typically scanned after being written on the article. The focus of this research is on offline signature verification, which presents unique challenges due to the lack of dynamic information.

Numerous methods have been developed to tackle the problem of signature verification. For online systems, approaches such as writer-specific feature extraction and classifiers have been proposed. For example, an approach leveraging Gaussian mixture models was introduced by Xia *et al.* to align signatures for improved matching [1]. Offline systems, on the other hand, primarily rely on the structural and geometric properties of the signature itself. Zhu *et al.* [2] proposed a method that captures the characteristic structural saliency of the signature for detection and segmentation purposes. Similarly, Hou *et al.* [3] developed an image descriptor for predicting human fixation points, which has been adapted for signature verification.

In recent years, deep learning approaches have gained popularity for signature verification. Alajrami *et al.* [4] introduced a convolutional neural network (CNN) model for offline verification, contrasting it with online techniques. Their work, along with that of Sudharshan and Vismaya [5], who evaluated CNN architectures like VGG16, VGG19, and ResNet50, demonstrated the potential of deep learning for this task. Moreover, Abdirahman *et al.* [6] explored advanced deep learning models such as MobileNet, ResNet50, and YOLOv5, aiming to improve the detection of forged signatures through better preprocessing and model architecture.

Despite the progress made, offline signature verification still faces significant challenges, particularly in terms of robustness to variations in handwriting and the complexity of forgeries. Many existing methods struggle to handle the intricacies of handwritten signatures, such as subtle distortions or variations that occur naturally between different instances of a genuine signature. Moreover, traditional deep learning methods often require large amounts of training data and substantial computational resources,

*** Corresponding author: Alireza Ataei,** Department of Mathematics, Faculty of Intelligent Systems Engineering and Data Science, Persian Gulf University, Bushehr, Iran, e-mail: ataei@pgu.ac.ir
Ebaa Abdulsattar Jaber: Department of Mathematics, College Of Education for Pure Sciences, University of Babylon, Babylon, Iraq, e-mail: edu792.a.abadalsataar@uobabylon.edu.iq
Ali Tavakoli: Department of Mathematics, University of Mazandaran, Babolsar, Iran, e-mail: a.tavakoli@umz.ac.ir

making them less practical for certain applications. The current methods, while effective to a certain degree, do not fully address the variability in offline signatures or the need for high accuracy in complex forgery detection. This study aims to fill this gap by introducing a novel approach that combines geometric properties of curves with advanced image processing techniques. Specifically, our method utilizes multiple knot B-splines in approximation theory, mean curvature analysis, and curve fitting to develop a comprehensive framework for signature verification. By leveraging these mathematical tools, our approach enhances the accuracy of distinguishing between genuine and forged signatures, even in cases where subtle variations exist. The validity of our results are confirmed by some examples.

2 Preliminaries

In this section, we introduce two basic concepts called skeleton of images and approximation of simple curves by b-splines, which are essential to our discussions in the next sections.

The skeleton of an image serves as a powerful tool for shape analysis. It simplifies the structure of an object by reducing its shape to a one-dimensional representation, capturing the essential geometric features while discarding the unnecessary details. This simplification facilitates various applications, including object recognition, image segmentation, and morphological operations, making the skeleton a cornerstone in the study of image topology and structure.

On the other hand, the approximation of simple curves by B-splines provides a robust framework for curve representation and manipulation. B-splines, or Basis splines, offer a flexible and mathematically sound method for approximating complex curves with a series of simpler, piecewise polynomial segments. This approach not only enhances the precision of curve modeling but also ensures smoothness and continuity, which are vital for applications in computer-aided design, animation, and geometric modeling. Together, these concepts form a foundation for advanced image processing techniques and geometric modeling, enabling more sophisticated and efficient solutions to problems in computer vision and graphics. In the following sections, we will explore the theoretical underpinnings, practical algorithms, and application scenarios for both the skeleton of images and the use of B-splines in curve approximation.

2.1 Skeleton of images

When the image of a signature is scanned on a page, usually lines or curves in the signature are saved as multi-pixel thickness. Therefore, the single-pixel skeleton of a signature can describe well the nature of it; hence, it had better consider the single-pixel skeleton of signatures. Thus, by verification of the skeletons of signature, we can evaluate the signature verification. Some techniques for skeletonization can be found in [7–9]. In Figure 1, some alphabet letters and their skeletons are seen.

2.2 Approximation of simple curves by b-splines

Some plane curves do not cross themselves, except probably in the end points. These curves are referred to as

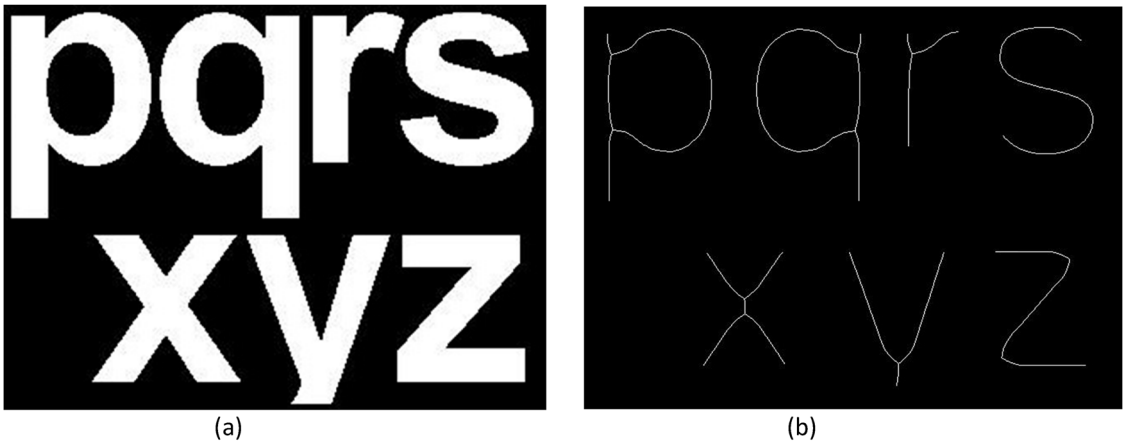

(a) (b)

Figure 1: Some alphabet letters (a) and their skeletons (b).

simple curves. A signature usually consists of some simple curves (Figure 2) that each one can be well simulated by b-splines [10,11]. Moreover, some signatures are undesirably involved small fluctuations that can be eliminated by b-splines (see Figure 7).

Definition 2.1. Consider the increasing knot vector $\mathbf{E} = \{t_i \le t_{i+1} \le \ldots \le t_{i+m}, i \in \mathbb{Z}\}$. For $m \ge 2$ and $t \in \mathbb{Z}R$, the ith b-spline basis function of order m is obtained from the following recursive definition:

$$B_{i,m,\mathbf{E}}(t) = \begin{cases} 0, & t_i = t_{i+m}, \\ s_1(t), & t_i < t_{i+m-1} \quad \text{and} \quad t_{i+1} = t_{i+m}, \\ s_2(t), & t_i = t_{i+m-1} \quad \text{and} \quad t_{i+1} < t_{i+m}, \\ s_1(t) + s_2(t), & \text{otherwise}, \end{cases}$$

where

$$s_1(t) = \frac{t - t_i}{t_{i+m-1} - t_i} B_{i,m-1,\mathbf{E}}(t),$$
$$s_2(t) = \frac{t_{i+m} - t}{t_{i+m} - t_{i+1}} B_{i+1,m-1,\mathbf{E}}(t)$$

and

$$B_{i,1,\mathbf{E}}(t) = \begin{cases} 1, & t_i \le t < t_{i+1}, \\ 0, & \text{otherwise}. \end{cases}$$

In Figure 3, the quadratic b-spline functions are shown that are constructed on the knot vector

$$\mathbf{E} = \left\{0, 0, 0, \frac{1}{5}, \frac{2}{5}, \frac{3}{5}, \frac{4}{5}, \frac{4}{5}, 1, 1, 1\right\}.$$

Explicit formulas of multiple knot b-splines for some special cases can be found in [12].

Definition 2.2. Given n points $d_1, \ldots, d_n$ and a knot vector $\mathcal{J} = \{t_1, t_2, \ldots, t_{n+m+1}\}$, where $t_1 \le t_2 \le \ldots \le t_{n+m+1}$, the **b-spline curve** defined by

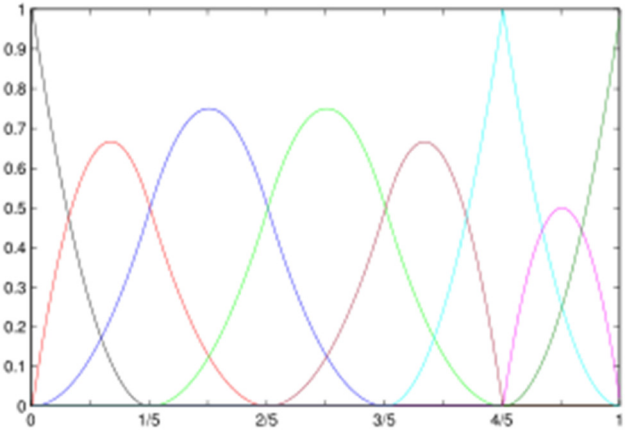

Figure 3: The quadratic b-spline functions defined at the knot vector $\mathbf{E} = \left\{0, 0, 0, \frac{1}{5}, \frac{2}{5}, \frac{3}{5}, \frac{4}{5}, \frac{4}{5}, 1, 1, 1\right\}$.

$$\mathbf{c}(t) = \sum_{i=1}^{n} d_i B_{i,m,\mathcal{J}}(t), \quad t \in [0, 1],$$

where $B_{i,m,\mathcal{J}}$'s are b-spline basis functions of order m. The vector-valued coefficients d_i's are referred to as **control points**.

The b-spline curves have continuous derivatives of order $m - 1$ (C^{m-1}-continuous). Repeating a knot k times in the nodal points decreases the number of continuous derivatives by k or the b-spline curves is C^{m-k-1}-continuous [11].

To simulate a curve *via* isogeometry techniques with multiple knot b-spline functions, it had better use the smooth b-spline functions with smallest degree [13,14]. In Figure 4, a signature and its simulation by b-splines of order $m = 3$ are shown on the knot vector $\mathbf{E} = \left\{0, 0, 0, \frac{1}{5}, \frac{2}{5}, \frac{3}{5}, \frac{4}{5}, \frac{4}{5}, 1, 1, 1\right\}$ and the control points $\{(0, 1), (1, 0), (2, 0), (2, 2), (4, 2), (5, 4), (2, 5), (1, 3)\}$.

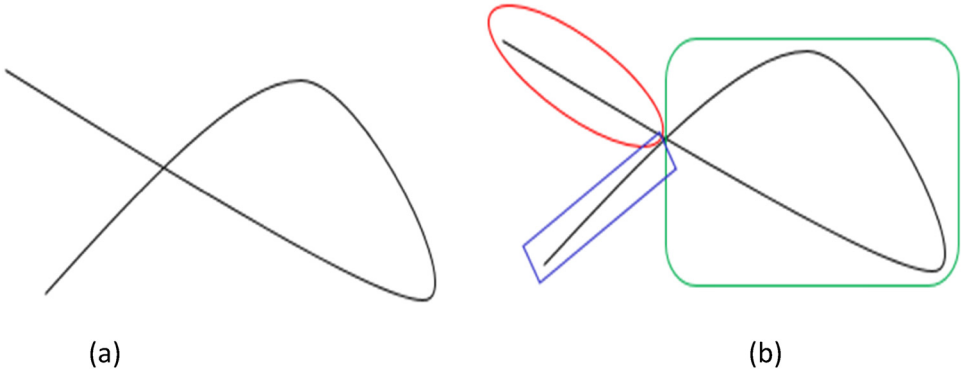

Figure 2: A signature (a) and its three simple curves (b).

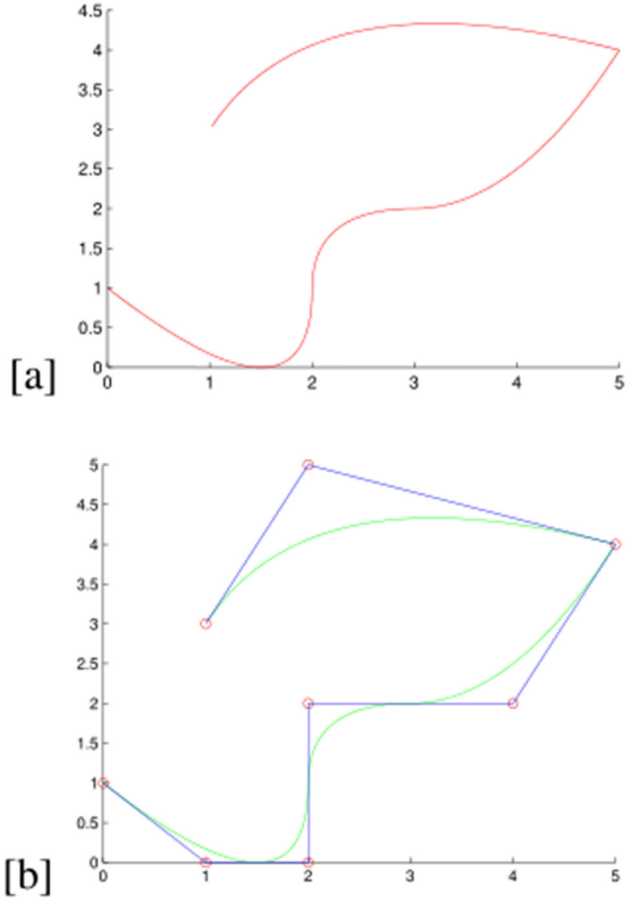

Figure 4: A signature (a) and its simulation by b-splines (b).

3 Methodology of signatures

In this section, we present an algorithm called signature line recognition (SLR) and image analysis techniques (IMAT) to verify the originality of a signature. We first consider the signature as an image. Also, we assume that an original signature of per person is in access. The steps of the following algorithm should be done for genuine and questioned signatures (GQSs). To determine the linear fitting curve (LFC) of a signature curve, we fit a line $y = ax + b$ to the points (x_i, f_i), $i = 1,\dots,n$. This line

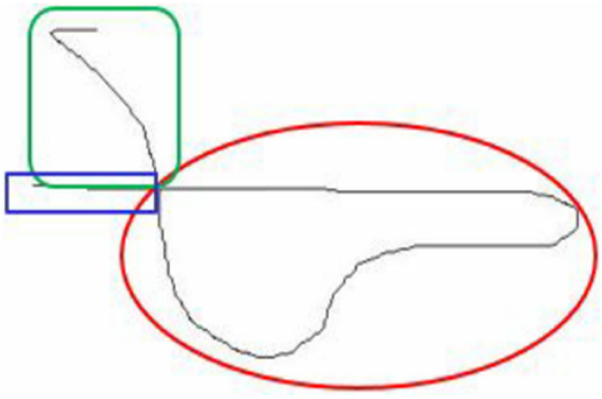

Figure 6: Three simple curves of a signature.

minimizes the distances from the points to the line. The parameters a and b are obtained by solving the following minimization problem:

$$\text{LFC} = \min_{a,b} \sum_{i=1}^{n} \frac{|ax_i + b - f_i|}{\sqrt{a^2 + b^2}}. \tag{1}$$

Algorithm 1. SLR-IMAT

Step 1: Extract the skeleton:
We extract a one pixel-width skeleton of the signature image. One pixelness of the width of the skeleton saves the time to find faster the originality of the signature.
Step 2: Find the number of simple curves.
Step 3: Smooth the skeleton curve of the signature.
The b-spline functions and isogeometry analysis can be used to remove small fluctuations (if any) the signature.
Step 4:
(a) Let $X_1,\dots, X_n$ be the points where the slope of signature curves change (critical points).
(b) Let $\kappa_1,\dots, \kappa_n$ be the curvatures of the signature curve in $X_1,\dots, X_n$, respectively.
(c) Compute the mean curvature as $\bar{\kappa} = \frac{1}{n}\sum_{i=1}^{n}\kappa_i$.
This step is important, because the curvature of a curve is invariant under transformation and rotation [15].

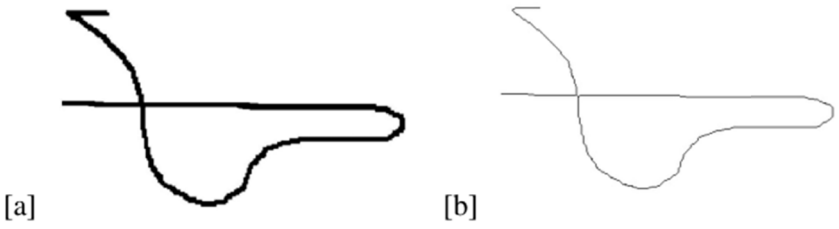

Figure 5: A signature (a) and its skeleton (b).

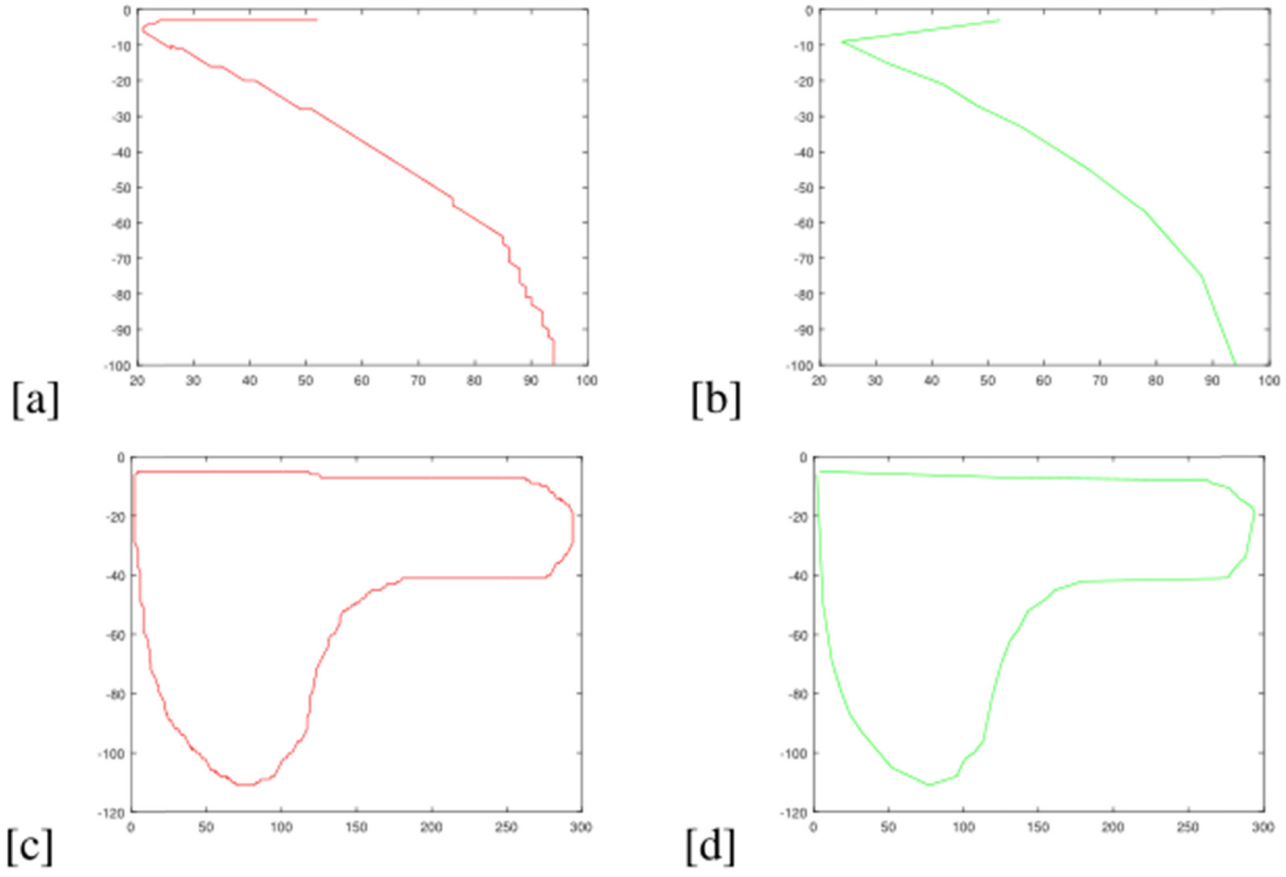

Figure 7: Two simple curves (a, c) and the corresponding smoothed curves (b, d).

Algorithm 1. SLR-IMAT

Step 5: Determine the linear fitting curve: The line $y = ax + b$ fits the points (x_i, f_i), $i = 1, \ldots, n$, of a signature curve where a and b are obtained by solving the minimization problem (1).

Theorem 3.2. [15] *The linear fitting of a curve, defined in Step 5, is invariant under transformation and rotation.*

The *accuracy* of a signature can be given by

$$\mathrm{AC}(f) = 1 - \frac{\sum_{i=1}^{3} w_i |N_i - N_i^*|}{\sum_{i=1}^{3} w_i (N_i + N_i^*)},$$

where $w_i > 0$, $i = 1, 2, 3$ are the weights of the given steps and are selected such that $w_1 + w_2 + w_3 = 1$. Moreover,

N_1^* and N_1 are the number of simple curves in the GQS's, respectively;

N_2^* and N_2 are the mean curvatures in the GQS's, respectively;

N_3^* and N_3 are the value of LFC for the GQS's, respectively.

Remark 3.3. in Algorithm 1, the effect of magnification on the signatures has been ignored. However, it is well known that if the magnification rate of the GQS's is K, then in

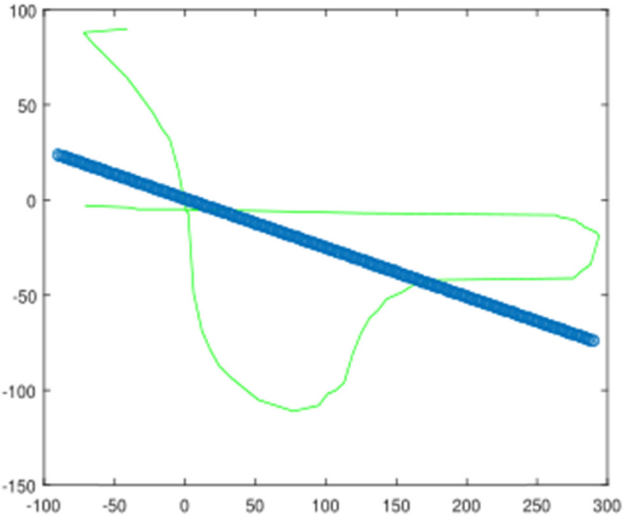

Figure 8: The linear fitting curve for the genuine signature given in Figure 5.

Figure 9: The questioned signature corresponding the genuine signature in Figure 5.

Algorithm 1, the LFC and the number of simple curves do not change, but the mean curvature changes $1/K$ times.

Table 2: The accuracy for Example 4.2

		Genuine	Questioned	AC(f)
Figures 10(a, b)	Number of simple curves	5	5	0.9699
	LFC	1.045	1.257	
	Mean curvature	0.339	0.523	
Figures 10(c, d)	Number of simple curves	9	4	0.5225
	LFC	5.065	1.404	
	Mean curvature	3.528	1.205	
Figures 10(e, f)	Number of simple curves	9	9	0.9218
	LFC	1.141	0.404	
	Mean curvature	1.098	0.205	
Figures 10(g, h)	Number of simple curves	13	11	0.8980
	LFC	0.820	1.146	
	Mean curvature	0.912	0.45	

4 Numerical experiments

In this section, by presenting some signatures, we verify their accuracy. In fact, the probability of originality for some signatures are given.

Example 4.1. Consider a genuine signature and its skeleton in Figure 5. It contains three simple curves (Figure 6). Based on Step 3, small fluctuation of the signature should be removed by b-splines (Figure 7). Next, according to Step 5, the LFC should be computed for the current genuine signature (Figure 8).

The aforementioned steps are done for both genuine (Figure 5) and questioned (Figure 9) signatures. For computing AC(f), the weights are chosen as $w_1 = w_2 = w_3 = 1/3$. Table 1 shows the mean curvatures and the error values of LFC for GQS's and the accuracy of the questioned signature. As is seen the questioned signature is original with the probability of 95%. Both signatures have the same number of simple curves (3), similar LFC errors (0.6868 for genuine and 0.3418 for questioned), and identical mean curvature values (0.0188). These closely matched characteristics result in a high accuracy of 0.9512, indicating a strong likelihood that the questioned signature is genuine. This example demonstrates the effectiveness of our method in accurately verifying signature authenticity by analyzing geometric properties.

Table 1: The accuracy for Example 4.1

	Genuine	Questioned	AC(f)
Number of simple curves	3	3	0.9512
LFC	0.6868	0.3418	
Mean curvature	0.0188	0.0188	

Example 4.2. In this example, we consider four genuine signatures with their corresponding questioned signatures. For all signatures the weights are taken as $w_1 = w_2 = w_3 = 1/3$. Table 2 shows the accuracy for all given signatures in Figure 10. Table 2 presents the accuracy AC(f) for four sets of genuine and questioned signatures, evaluated using the number of simple curves, LFC error, and mean curvature, with equal weights $w_1 = w_2 = w_3 = \frac{1}{3}$. For the signatures in Figure 10(a, b), both have 5 simple curves, similar LFC errors, and mean curvatures, resulting in a high AC(f) = 0.9699. In Figure 10(c, d), significant differences in all metrics yield a lower AC(f) = 0.5225. Figure 10(e, f) show matching numbers of simple curves and similar metrics, resulting in AC(f) = 0.9218. Finally, Figures 10(g, h) display close values in all metrics, leading to AC(f) = 0.8980. These results illustrate that closer metric values between genuine and questioned signatures correspond to higher accuracy, indicating stronger matches.

Example 4.3. For the last example, we compare our proposed method with several other methods on the database provided by [16]. This database contains 800 genuine and questioned signature images across 20 classes, with 40 signatures in each class. In this database, two criteria, the false rejection rate (FRR) and the false acceptance rate (FAR), are reported for genuine and questioned signatures, respectively. In [2,16,17], they considered the first 20

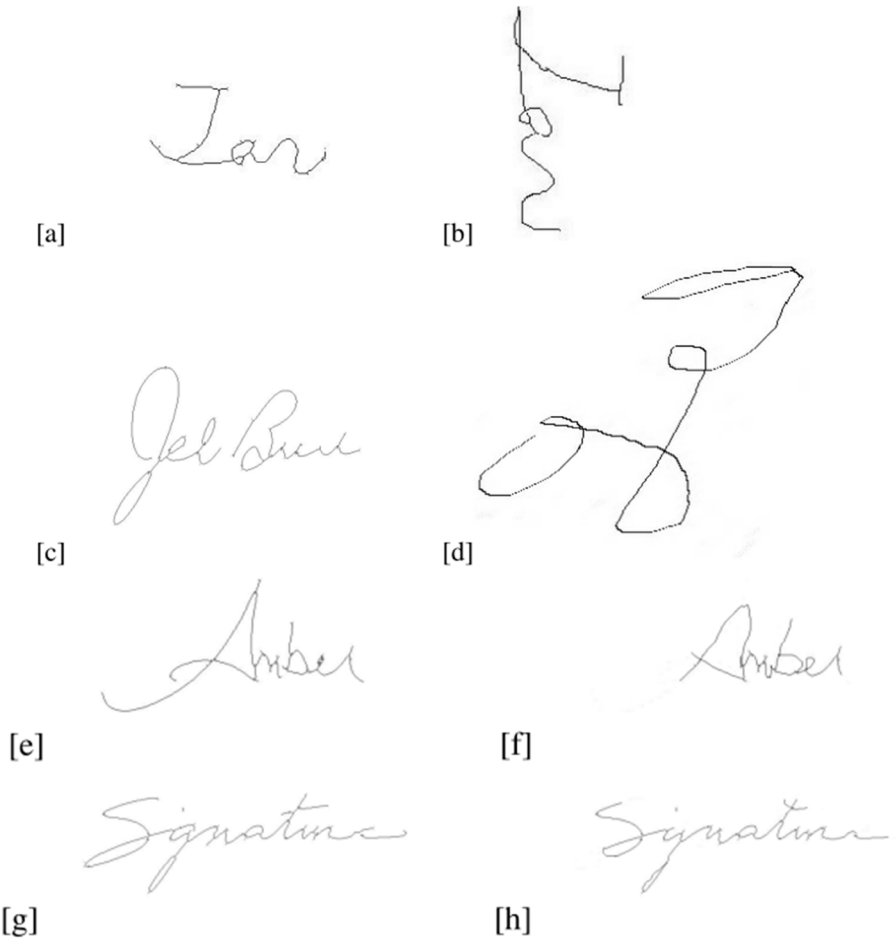

Figure 10: The GQS's of the Example 4.2.

signatures in each class for training and the second 20 signatures for testing. In our case, we do not have training data, so we only consider the test signatures. The results are presented in Table 3. As can be seen, our approach, with a FRR of 0.43% and a FAR of 0.18%, shows the best offline signature verification results on this database.

5 Conclusion

In this study, we introduced a novel algorithm for verifying the authenticity of signatures with high accuracy. Our approach combines geometric properties of curves, such as the number of simple curves, LFC error, and mean curvature, with advanced image processing techniques. By leveraging multiple knot B-splines in approximation theory, we developed a robust framework that effectively distinguishes between genuine and forged signatures.

The core of our method involves analyzing the skeleton of the signature image and computing specific geometric properties to determine the accuracy of the signature. Our empirical results, as presented in Table 2, demonstrate that our algorithm significantly improves accuracy in signature verification compared to existing methods. For instance, signatures with closer metric values between genuine and questioned samples exhibited higher accuracy, indicating stronger matches.

This research contributes to the field of signature verification by providing a comprehensive and reliable method for signature authentication. The success of our algorithm in various empirical examples suggests its

Table 3: Comparison of FRR and FAR for signature database given in [16]

Method	FRR (%)	FAR (%)
Sabourin *et al.* [16]	1.64	0.10
Shanker and Rajagopalan [18]	8.75	3.26
Guo *et al.* [17]	1.66	1.10
Zhu *et al.* [2]	0.5	0.21
Our approach	0.43	0.18

potential for broader applications in legal, financial, and security contexts. Furthermore, our findings open avenues for future studies to enhance and adapt our algorithm, potentially incorporating additional features or refining the current ones to further improve its effectiveness in diverse scenarios.

Funding information: Authors state no funding involved.

Author contributions: All authors contributed to the study's conception and design. The manuscript was written, reviewed, and approved by all authors in the order presented on the first page of the manuscript.

Conflict of interest: The authors declare no conflicts of interest related to this research.

Data availability statement: All data generated or analysed during this study are included in this published article.

References

[1] Xia X, Chen Zh, Luan F Song X. Signature alignment based on GMM for on-line signature verification. Pattern Recognition. 2017;65:188–96.
[2] Zhu G, Zheng Y, Doermann D, Jaeger S. Signature detection and matching for document image retrieval. IEEE Trans Pattern Anal Machine Intel. 2008;31(11):2015–31.
[3] Hou X, Harel J, Koch C. Image signature: highlighting sparse salient regions. IEEE Trans Pattern Anal Machine Intel. 2011;34(1):194–201.
[4] Alajrami E, Ashqar BAM, Abu-Nasser BS, Khalil AJ, Musleh MM, Barhoom AM, et al. Handwritten signature verification using deep learning. Int J Academic Multidiscipl Res. 2019;3(12):39–44.
[5] Sudharshan DP, Vismaya RN. Handwritten signature verification system using deep learning. IEEE International Conference on Data Science and Information System (ICDSIS). Hassan, India; 2022. p. 1–5.
[6] Abdirahma AA, Hashi AO, Elmi MA, Rodriguez OER. Advancing handwritten signature verification through deep learning: a comprehensive study and high-precision approach. Int J Eng Trends Tech. 2024;72(4):81–91.
[7] Barbieri S, Meloni P, Usai F, Spano LD, Scateni R. An interactive editor for curve skeletons. Comput Graphics. 2016;60:23–33.
[8] Cai Y, Ming Ch, Qin Y. Skeleton extraction based on the topology and Snakes model. Results Phys. 2017;7:373–8.
[9] Saha PK, Borgefors G, Baja GSD. A survey on skeletonization algorithms and their applications. Pattern Recognition Lett. 2016;76:3–12.
[10] Schumaker L. Spline functions: basic theory. 3rd ed. Cambridge: Cambridge University Press; 2007.
[11] Zarmehi F, Tavakoli A. Construction of the matched multiple knot B-spline wavelets on a bounded interval. Int J Comput Math. 2015;92(8):1688–714.
[12] Esmaeili M, Tavakoli A. Construction of new multiple knot B-spline wavelets. Rocky Mountain J Math. 2017;47(5):1463–95.
[13] Cottrell JA, Hughes TJR, Bazilevs Y. Isogeometric analysis: toward integration of CAD and FEA. John Wiley and Sons; 2009.
[14] Tavakoli A, Zarmehi F. Construction of the matched multiple knot B-spline wavelets on a bounded interval. Int J Comput Math. 2015;92(8):1688–714.
[15] Kimmel R. Numerical geometry of images: theory, algorithms, and applications. Verlag New York: Springer; 2004.
[16] Sabourin R, Genest G, Preteux F. Off-line signature verification by local granulometric size distributions. IEEE Trans Pattern Anal Machine Intel. 1997;19(9):976–88.
[17] Guo K, Doermann D, Rosenfeld A. Forgery detection by local correspondence. Int J Pattern Recognit Artif Intel. 2001;15(4):579–641.
[18] Shanker A, Rajagopalan A. Off-line signature verification using DTW. Pattern Recognit Lett. 2007;28(12):1407–14.